Published in final edited form as:
J Neurochem. 2012 December ; 123(5): 689–699. doi:10.1111/j.1471-4159.2012.07918.x.

Decreases in Plasma Membrane Ca^{2+}-ATPase in Brain Synaptic Membrane Rafts from Aged Rats

Lei Jiang[1], **Misty D. Bechtel**[1], **Nadezhda A. Galeva**[2], **Todd D. Williams**[2], **Elias K. Michaelis**[1], and **Mary L. Michaelis**[1]

[1]Department of Pharmacology and Toxicology and Higuchi Biosciences Center, The University of Kansas, Lawrence, KS 66047, USA

[2]Analytical Proteomics Laboratory, Structural Biology Center, The University of Kansas, Lawrence, KS 66047, USA

Abstract

Precise regulation of free intracellular Ca^{2+} concentrations $[Ca^{2+}]_i$ is critical for normal neuronal function, and alterations in Ca^{2+} homeostasis are associated with brain aging and neurodegenerative diseases. One of the most important proteins controlling $[Ca^{2+}]_i$ is the plasma membrane Ca^{2+}-ATPase (PMCA), the high affinity transporter that fine tunes the cytosolic nanomolar levels of Ca^{2+}. We previously found that PMCA protein in synaptic plasma membranes (SPMs) is decreased with advancing age and the decrease in enzyme activity is much greater than that in protein levels. In the present study, we isolated raft and non-raft fractions from rat brain SPMs and used quantitative mass spectrometry to show that the specialized lipid microdomains in SPMs, the rafts, contain 60% of total PMCA, comprised of all four isoforms. The raft PMCA pool had the highest specific activity and this decreased progressively with age. The reduction in PMCA protein could not account for the dramatic activity loss. Addition of excess CaM to the assay did not restore PMCA activity to that in young brains. Analysis of the major raft lipids revealed a slight age-related increase in cholesterol levels and such increases might enhance membrane lipid order and prevent further loss of PMCA activity.

Keywords

PMCA; brain aging; calcium; synaptic rafts; protein mass spectrometry; calmodulin

Introduction

Transient increases in free intracellular Ca^{2+} serve as signals in critical neuronal processes such as neurotransmitter release, energy metabolism, synaptic plasticity, and gene transcription essential for learning and memory (Berridge 1998; Blackstone and Sheng 2002). The cytosolic Ca^{2+} must be rapidly returned to normal resting levels following Ca^{2+} transients and maintained in the nanomolar concentration range through the activities of Ca^{2+} transporters and binding proteins. Aberrant cellular Ca^{2+} overload has been implicated in neuronal dysfunction occurring in brain aging (Huidobro et al. 1993; Khachaturian 1994; Camandola and Mattson 2011) and in neurodegenerative disorders such as Alzheimer's disease (Khachaturian 1994; Mattson 2007; Camandola and Mattson 2011), and Parkinson's disease and stroke (Mattson 2007). The aging process in brain is accompanied by a higher

Address correspondence to: Mary L. Michaelis, Higuchi Biosciences Center, 2099 Constant Avenue, The University of Kansas, Lawrence, Kansas 66045, Phone: 785-864-3905, Fax: 785-864-5738, mlm@ku.edu.

The authors have no conflicts of interest to declare.

overall Ca^{2+} content in brain neurons and synaptic terminals and a slower clearance of Ca^{2+} from nerve endings following a depolarizing stimulus (Martinez et al. 1988; Michaelis et al. 1992).

The calmodulin (CaM)-activated plasma membrane Ca^{2+}-ATPase (EC 3.6.3.8) or PMCA is the major high-affinity, low-capacity Ca^{2+} extrusion system at the plasma membrane. Four isoforms of PMCA have been identified and form a multi-gene family with numerous splice variants that are selectively expressed in various tissues and presumably control diverse and highly regulated functions within a given type of cell (Strehler and Zacharias 2001). By pumping excess cytosolic Ca^{2+} into the extracellular space, PMCA is partly responsible for the long term regulation of resting free intracellular Ca^{2+} concentrations and reversing transient increases that occur during Ca^{2+} signaling (Strehler and Zacharias 2001; Clapham 2007). The PMCA levels and ATPase activity in brain synaptic membranes have been found to decrease with brain aging, an observation that could, at least partially, explain the age-associated elevations in intra-neuronal free Ca^{2+} (Gibson and Peterson 1987; Martinez et al. 1988; Michaelis et al. 1992) and the slower decay of Ca^{2+} transients in intact synaptosomes (Martinez-Serrano et al. 1992) and in hippocampal neurons (Landfield and Pitler 1984) from aged F344 rats. We had previously observed that both Ca^{2+}-ATPase and the ATP-dependent Ca^{2+} transport activity in synaptic plasma membranes (SPMs) prepared from brains of aged Fisher 344 rats was significantly lower than that in young animals (Michaelis et al. 1984; Michaelis 1989). We further confirmed the progressive age-dependent decrease in PMCA activity in the longer-lived Fisher 344/BNF1 hybrid rat strain. The V_{max} for activity in SPMs isolated from 34 month old rats was 48% lower than that at 5 mos, and this decrease was only partially due to a reduction in PMCA protein levels in the SPMs (Zaidi et al. 1998). In addition to the 20% reduction in PMCA levels, the amount of CaM present in the membranes was reduced by approximately 30%. However, the addition of saturating amounts of exogenous CaM did not overcome the progressive decrease in the PMCA activity measured in SPMs from the aged rats.

Several lipids are known to regulate PMCA activity, and the activating effect of acidic phospholipids is even more pronounced than that of CaM (Di Leva *et al.* 2008). The activity of PMCA is quite sensitive to the biophysical properties of the surrounding lipid environment, and the transporter exhibits much higher activity when it is localized in regions of ordered lipids (Duan et al. 2006; Tang et al. 2006). A portion of the PMCA in SPMs partitions into lipid ‘rafts’ (Sepulveda et al. 2006; Jiang et al. 2007), highly ordered micro-domains within the plasma membrane that are enriched in cholesterol, saturated phospholipids, and sphingolipids such as GM1 ganglioside (Brown and London 1997; Lucero and Robbins 2004). The rafts are involved in signal transduction by acting as a scaffold for protein sorting and promoting protein-lipid and protein-protein interactions (Simons and Toomre 2000) as exemplified in synaptic membranes (Hering et al. 2003; Gil et al. 2006). Cholesterol plays a key role in supporting the tendency of saturated phospholipids and sphingolipids to segregate from unsaturated phospholipids in the bilayer membrane (Silvius 2003), suggesting that altered cholesterol levels likely influence the activity of proteins such as PMCA within the raft domains.

The aims of the present study were: (1) to assess the partitioning of PMCA isoforms into raft and non-raft domains isolated from brain SPMs, (2) to determine the specific activity of the PMCA associated with the raft *vs* that present in the non-raft domains, (3) to assess the effects of aging on the specific activity of the PMCA within the raft domains of the SPMs, and (4) to assess the levels of CaM, cholesterol and ganglioside GM1 in the rafts with increasing age as possible contributors to the age-dependent decrease in PMCA activity seen in intact SPMs. In the present study, we used quantitative liquid chromatography-mass spectrometry (LC-MS/MS) to assess the relative enrichment of PMCA isoforms in raft

domains isolated from synaptic membranes. We also examined the constants (V_{max} and K_{act}) for the activity of PMCA in raft and non-raft domains and determined the presence and activity of CaM remaining tightly bound to the lipid rafts. Following such characterization of the lipid rafts and of the PMCA associated with these lipid microdomains, we focused on the effects of increasing age on cholesterol, GM1, PMCA, and CaM content in rafts, and on the activity of PMCA associated with rafts.

Materials and Methods

Materials

*S*ources for the various primary antibodies were as follows: anti-Flotillin-1 (FLT-1) and anti-Thy-1 (BD Biosciences), anti-CaM (Millipore), pan anti-PMCA (Affinity Bioreagents). Alkaline phosphatase-conjugated secondary antibodies, ficoll, ouabain, thapsigargin, oligomycin, ATP, Brij 98, and horseradish peroxidase-coupled cholera toxin subunit B (CTXB) were purchased from Sigma. The Amplex Red cholesterol assay kit and gradient gels (8–16%) were obtained from Invitrogen, the bicinchoninic acid protein assay reagents from Pierce Biotechnology, and the polyvinylidene fluoride (PVDF) membranes from Millipore. The protease inhibitor cocktail III and purified bovine brain CaM were purchased from Calbiochem.

Animals

Fisher 344/Brown Norway hybrid (F344/BNF1) male rats at 6, 23, and 34 months of age were obtained from the National Institute on Aging colony maintained by Harlan Industries. All protocols were implemented in accordance with NIH guidelines and approval by the University of Kansas Institutional Animal Care and Use Committee (IACUC). The rats were quarantined for 2 weeks after their arrival, following which they were used for the studies.

Isolation of SPMs and SPM rafts from rat brains

Fisher 344/BNF1 rats were anesthetized by CO_2 inhalation according to the IACUC guidelines. Rats were decapitated using a guillotine and the brains recovered quickly. The brains from one rat at each of the 3 ages were processed in parallel. Argon was bubbled through all solutions to eliminate O_2. Each whole brain was homogenized and processed immediately for the isolation of synaptosomes by discontinuous ficoll density gradient centrifugation as previously described (Michaelis et al. 1983; Jiang et al. 2010). The synaptosomes recovered from the gradient were lysed in a hypotonic buffer (3mM Tris-HCl, pH 8.5) containing a cocktail of protease inhibitors and centrifuged at 64,200 × *g* for 15 min. The SPM pellet was homogenized in buffer containing 10 mM Tris-HCl, 50 μM $MgCl_2$, and 0.32 M sucrose, pH 7.4. Lipid rafts were isolated from SPMs using discontinuous sucrose density gradient centrifugation essentially as described (Jiang *et al.* 2007). Briefly, the SPMs from each animal were solubilized in an equal volume of solubilization buffer (50 mM Tris-HCl, 150 mM NaCl, pH 7.5, containing 2% Brij 98), to achieve 1% Brij 98 as the final concentration, and incubated on ice for 30 min. The suspension was mixed 1:1 with a 90% sucrose solution and the resultant mixture overlaid with 35% and 5% sucrose solutions. Ultracentrifugation was performed for 18 h at 98,300 × *g* in a Beckman Optima Max centrifuge in an MLS-50 rotor. Ten fractions (0.4 ml each) were collected from the top to the bottom of each tube. However, due to the negligible amount of protein in fraction 1 and the small pellet of fraction 10 at the bottom of the tube, only fractions 2 – 9 were used in these experiments. Protein concentrations of the fractions were determined using the bicinchoninic acid assay according to the manufacturer's instructions. In order to compare the raft fractions with the non-raft domains, we pooled the fractions into 3 groups. Based on the relative levels of cholesterol, GM1, and Flotillin-1, fractions #2 – 4 were pooled as the

lipid raft microdomains. Fractions #5–6 and #7–9 were considered to be the higher density non-raft components of the SPMs.

Cholesterol and GM1 analysis

Cholesterol was measured using the Amplex Red cholesterol assay kit, and GM1 ganglioside levels were determined by immunoblotting using cholera toxin subunit B (CTXB) at 300 μg/ml. Briefly, an 8 μg protein aliquot from each fraction was separated by sodium dodecyl sulfate-polyacrylamide gel electrophoresis (SDS-PAGE), transferred to a PVDF membrane, blocked with 1% bovine serum albumin (BSA) for 30 min, and exposed to CTXB for 2 h. Color was developed by incubation in a mixture of 1.4 mM 3,3′-diaminobenzidine tetrahydrochloride, 200 mM NiCl and 6.2 mM H_2O_2. Based on the levels of cholesterol and GM1 ganglioside associated with the various fractions, the contents of specific fractions were pooled into 3 groups: fraction #2–4, #5–6, and #7–9. These 3 groups were analyzed.

Immunoblot Analysis

Proteins were separated by SDS-PAGE and transferred to PVDF membranes as we have described previously (Jiang *et al.* 2007). Non-specific interactions were blocked with 5% (w/v) milk solution for 1 h at 25°C and the membranes incubated overnight with the indicated concentrations of primary antibodies. Alkaline phosphatase-conjugated secondary antibodies (1:1000) were added for 2 h at 25°C. Immunoblots were developed using the substrate 5-bromo-4-chloro-3-indoyl phosphate and nitroblue tetrazolium. Blots were scanned using a Kodak Image Station 4000MM PRO and quantified using Carestream Molecular Imaging Software 5.x.

Capillary liquid chromatography- mass spectrometry (LC-MS/MS) analysis of PMCA isoforms

Protein samples from pooled fractions # 2–4, #5–6, and #7–9 were run on SDS-PAGE gels and stained with Coommassie blue. Gel pieces at the molecular weight range of PMCA were excised, the proteins within the slices reduced with dithiothreitol, alkylated with iodoacetamide, and digested (37 °C, overnight) with 0.25 μg of trypsin in 0.2 M NH_4CO_3 - 5% acetonitrile (ACN). Ten microliter peptide-containing samples were analyzed by LC-MS/MS using a NanoAcquity chromatographic system (Waters Corp.) coupled to an LTQ-FT mass spectrometer (ThermoFinnigan). The peptides were separated on a C_{18} column (5cm, 300 μm I.D.; Thermo Acclaim PepMap300; flow rate 10 μL/min) using a gradient 1 – 40% of solvent B (99.9% ACN, 0.1% formic acid) developed over 50 min, ramped to 95% solvent B over 4 min, and held at 95% for 5 min. Solvent A was 99.9% H_2O, 0.1% formic acid. A NanoAquity UPLC Console (Waters Corp., version 1.3) was used to execute the injections and gradients. The ESI source was operated with spray voltage of 2.8 kV, a tube lens offset of 160 V, and a capillary temperature of 200 °C. All other source parameters were optimized for maximum sensitivity of the YGGFL peptide MH^+ ion at m/z 556.27. The instrument was calibrated using an automatic routine based on a standard calibration solution. Data acquisition via LTQ-FT was set up using Xcalibur software (ThermoElectron Corp., version 2.0.7). Full MS survey scans were acquired at a resolution of 50,000 with an Automatic Gain Control (AGC) target of 5×10^5. The LTQ-FT Selected Ion Monitoring (SIM) scan sequence was adapted from that described (Olsen and Mann 2004).

MS/MS spectra were analyzed using Mascot (Matrix Science, 2.3), Sequest (Thermo Fisher Scientific, 27, rev. 12), and X! Tandem (The GPM, thegpm.org; CYCLONE (2010.12.01.1)). Search engines were set up to search the IPI_rat database (v. 3.87, 39925 entries) or Swiss-Prot database (only rattus taxonomy), assuming digestion by trypsin and allowing for 2 missed cleavages. Fragment ion mass tolerance of 0.20 Da and a parent ion

tolerance of 20 ppm were used. The iodoacetamide derivative of cysteine was specified as a fixed modification, while oxidation of methionine was designated a variable modification. Scaffold software (Scaffold_3_4, Proteome Software Inc.) was used to validate MS/MS based peptide and protein identifications. The SIM acquisition method for the LTQ-FT was adopted based on the results of LC-MS/MS experiments to achieve better sensitivity and to focus on the four selected, PMCA isoform-specific peptides with significant sequence homology: GIIDSTVSEQR for PMCA1, GIIDSTHTEQR for PMCA2, GIIDSTTGEQR for PMCA3, GIIDSNIGEQR for PMCA4 (see also Table 1, Supplementary Material). FT SIM experiments were set to scan the m/z range of 626.30–631.30 from 10.0 to 12.6 min, of 586.30–591.30 from 12.6 to 15.2 min, of 600.32–605.320 from 15.2 to 17.2 min, and of 598.82–603.82 from 17.2 to 20.2 min. FT SIM scans were acquired at a resolution of 100,000 with an AGC target of 2×10^5 or maximum ion time of 1.2 s. The chromatographic peaks were integrated using Qual Browser of Xcalibur software. FT SIM peak areas were used for reporting quantitative stoichiometric ratios of PMCA isoforms in samples thus analyzed.

Measurement of PMCA activity

The PMCA activity was determined at 37ºC by monitoring the generation of Pi from the hydrolysis of ATP as described previously (Zaidi et al. 1998; Jiang et al. 2007). The assay was conducted in a final volume of 100 μL containing 3μg sample protein, 25 mM Tris-Cl, pH 7.4, 50 mM KCl, 1 mM ATP, 1 mM $MgCl_2$, 0.1 mM ouabain, 4 μg/mL oligomycin, 0.1 μM thapsigargin, 200 μM EGTA, and $CaCl_2$ at different concentrations added to yield the final free Ca^{2+} concentrations indicated in the figures. The final free Ca^{2+} concentration was calculated using the software calcium.com that calculates the multiple equilibria between all ligands in solution. During their preparation, the synaptic membranes were not exposed to chelators to extract the endogenous CaM bound to them. Thus the PMCA activity was measured in the presence of the CaM already associated with the membranes except in the experiments in which it was noted that a saturating amount of exogenous CaM was added to the assay. After a 5 min pre-incubation, the reaction was initiated by the addition of ATP, continued for 30 min at 37°C, and stopped by addition of the Malachite Green dye solution (Lanzetta *et al.* 1979). The absorbance was measured immediately at 650 nm. The specific activity of PMCA was defined as the nmoles of Pi liberated per mg of protein per min.

Statistical Analyses

The statistical significance of differences between samples were determined by Student's *t*-test for unpaired samples or by ANOVA, whichever was more appropriate for the type of data being analyzed.

Results

Characterization of lipid rafts isolated from rat brain SPMs

Lipid rafts were isolated from SPMs prepared from the individual brains of 6, 23, and 34 mos F344/BNF1 rats using the non-ionic detergent Brij 98 at a final concentration of 1% (v/v). Only the brains of 6 month-old rats were used in the initial characterization of the rafts and the partitioning of the PMCA in raft and non-raft domains. After the sucrose density gradient centrifugation, fractions 2–9 were collected from the top to the bottom of the tube as noted in the Methods. Cholesterol, one of the major lipid markers of rafts, was significantly enriched in the low-density fractions, #2–4. The cholesterol content in these fractions represented 77.4 ± 0.9% of the total cholesterol in the membranes applied to the gradient (Fig. 1A). Cholesterol was substantially more enriched in fractions #2–4 than proteins were. These fractions contained 31.6 ± 1.2% of the total protein in the SPMs. An additional lipid raft marker, GM1 ganglioside, was highly enriched in fractions #2–4, as

were two raft protein markers, Thy-1 and FLT-1 (Fig. 1B), consistent with our previous observations (Jiang et al. 2010). Figure 1B also shows the distribution of PMCA in the raft and non-raft fractions based on an immunoblot analysis with the pan-PMCA antibody. Densitometric analyses of the total PMCA immunoreactivity in fractions #2 to #9 indicated that a greater percentage of the total amount of PMCA was associated with the detergent-resistant, low density fractions #2–4 than with fractions #5–6 or #7–9 (data not shown).

To quantify the levels of total PMCA and of each of the four isoforms of the enzyme in the three pooled fractions, we performed quantitative MS analyses of these fractions as described under *Methods*. Liquid chromatography-MS/MS analysis of the in-gel digested samples followed by database searches identified the presence of all four PMCA isoforms, as well as that of many other proteins, in the gel slices excised from the region corresponding to the molecular sizes of the PMCA isoforms. Sequence coverage for each PMCA isoform was in the range of 15–20% and a total number of 45 peptides were assigned to PMCA isoforms with greater than 50% probability as specified by the Peptide Prophet algorithm (Keller et al. 2002). There were 8, 12, 5, and 12 isoform-specific peptides (including the ones with probability less than 50%) detected by MS/MS and assigned to PMCA isoforms 1, 2, 3, and 4, respectively (Tables 2–5 Supplementary Material). PMCA isoform sequence alignment (Scheme 1, Supplementary Material) indicated a region of similarity within four isoform-specific peptides (Table 1, Supplementary Material). These peptides have 8 out of 11 residues in common across the four isoforms and were selected for further quantitative FT SIM MS experiments. The analysis of pooled samples from fractions #2–4, #5–6, and #7–9, using FT SIM MS allowed us to increase sensitivity for the PMCA representative peptides relative to full scan FT MS experiments. Stoichiometric ratios of PMCA isoforms were calculated by normalizing the FT SIM isoform-specific peptide signal to the sum of signals from the four selected peptides. This was achieved by focusing the mass spectrometer on a particular ion during the expected time.

The results of such analyses were averaged and are presented in figure 2 and Table 1. The data obtained indicated that ~60% of the total PMCA partitioned into the pooled raft fractions #2–4, and ~21% and ~19% partitioned into pooled fractions #5–6 and #7–9, respectively (Fig. 2A). The content of PMCA proteins in raft fractions (~60%) was nearly twice that of the total membrane protein distributed in those fractions (~31%, see Fig. 1A), an indication of selective association of PMCA with rafts. Quantitative MS analyses also revealed that of the four PMCA isoforms, PMCA 1, 2, and 4 were the most abundant isoforms in all of the fractions as determined by quantitative MS (Fig. 2B). The stoichiometric ratios of the four isoforms in each of the three pooled fractions are shown in Table 1.

As the final step in characterizing the raft and non-raft fractions, we determined the K_{act} and V_{max} values of the basal PMCA activity across Ca^{2+} concentrations in each of the 3 pooled fractions isolated from SPMs of 6 mos old rats. These studies were performed in the absence of exogenous CaM additions. We found that the specific activity of the enzyme was significantly higher in the raft fractions than in either of the pooled non-raft fractions (Fig. 3). The estimated V_{max} in the rafts was ~2.6-fold ($p<0.001$, Student t-test) and ~4.6-fold ($p<0.001$) higher than the V_{max} values in fractions #5–6 and #7–9, respectively (Table 2). The calculated values for the estimated K_{act} for Ca^{2+} for fractions #2–4 did not differ significantly from those for fractions #5–6 ($p=0.35$) and #7–9 ($p=0.52$). The K_{act} values for all fractions were similar to those observed previously for isolated SPMs (Zaidi et al. 1998) and were indicative of a high affinity state of PMCA for free Ca^{2+}.

The high affinity for Ca^{2+} in these preparations might be indicative of substantial amounts of CaM remaining bound to the three pooled fractions isolated from synaptic membranes.

The present measurements were obtained using preparations that were not treated with chelators, such as EDTA, to extract endogenous CaM; thus the V_{max} and K_{act} estimates probably reflected those of PMCA activated by any CaM remaining in association with the isolated fractions. The addition of exogenous CaM (300 nM) had no significant effect ($p>0.10$, t-test comparisons) on either the estimated V_{max} or the K_{act} for Ca^{2+}-induced activation of PMCA (Table 2). The lack of an effect by excess exogenous CaM on PMCA activity would be expected if substantial amounts of CaM remained bound to these fractions.

To assess the contribution of endogenous CaM to the activity of PMCA measured in the raft fractions, we pursued two approaches. The first was to pretreat the rafts with either of two CaM inhibitors, calmidazolium (10 μM) or trifluoperazine (50 μM). The second was to treat synaptosomes and SPMs with EDTA prior to isolation of the raft and non-raft fractions in order to extract CaM that might be tightly bound to components of the isolated fractions. Both types of treatments caused a reduction in PMCA activity in rafts of approximately 30–40%. This is demonstrated in figure 4A for the effect of calmidazolium on the PMCA activity of the pooled fractions #2–4. Calmidazolium caused a significant decrease ($p=0.005$, t-test) in the V_{max} of PMCA activity in the raft fractions and a 2.7-fold, but not significant ($p=0.098$), increase in the K_{act} for Ca^{2+} (Fig. 4A). The effects of calmidazolium on both V_{max} and K_{act} were completely reversed by the addition of 300 nM CaM (Fig. 4A). The effects of inhibitors of CaM on the PMCA activity in the raft fractions were indicative of the presence of endogenous CaM remaining associated with these preparations. When 3 mM EDTA was introduced during the lysis of synaptosomes and the isolation of synaptic membranes, it led to the extraction of ~48% of the CaM that was associated with the raft fractions but did not completely remove all CaM from those fractions (Fig. 4B). Because of the residual CaM in these fractions even following Ca^{2+} chelation, the precise level of contribution of CaM to the overall PMCA activity in rafts could not be accurately estimated, but it was obviously significant.

Effects of aging on PMCA protein levels and PMCAactivity in raft microdomains

Analysis of the levels of GM1 in SPM rafts from rats at 6, 23, and 34 mos revealed no significant age-related changes in this marker of raft domains in membranes. The total protein in the three pooled fractions as well as the levels of the protein raft markers, Thy-1 and FLT-1, also did not change with increasing brain age (data not shown). On the other hand, there was a small but statistically significant and progressive increase in the cholesterol to protein ratio in the rafts from the 23 mos and the 34 mos compared to the 6 mos old animals as shown in Fig. 5A.

The levels of the PMCA protein in rafts (fractions #2–4) were compared at the three ages in order to determine if there was any significant change in PMCA in rafts. To address the possibility that changes in raft PMCA levels during the aging process might result from altered distribution of PMCA in membranes, i.e., decreases in PMCA associated with the rafts and increases in PMCA in the non-raft domains, we also examined the effects of the aging process on the levels of PMCA in fractions #5–6 and #7–9. As shown in figure 5B, we observed a significant age effect on PMCA levels in rafts ($p=0.03$, ANOVA) and significant decreases for both the 23 and 34 mos raft fractions compared with the levels at 6 mos ($p<0.03$, t-test).

The same as described above for 6 mos old rats analyzed by quantitative MS and immunoblots (e.g., Fig. 2), the overall levels of PMCA in rafts isolated from 6 and 23 mos old rat brains were significantly higher ($p<0.01$, t-test) than those in fractions #5–6 and #7–9 (Fig. 5B). It should be noted that there was no significant age effect on the PMCA levels in the non-raft fractions. Therefore, it was unlikely that the decreases in PMCA levels in rafts were the result of re-distribution of the protein from the raft to the non-raft domain during

the aging process. Because of the lack of a change in PMCA levels in fractions #5–6 and #7–9, the focus of studies related to PMCA activity was primarily on the effects of aging on the raft fractions.

When the activity of PMCA was determined across Ca^{2+} concentrations in rafts isolated from SPMs of rats at 6, 23, and 34 mos of age, the estimated V_{max} decreased progressively and significantly with increasing age of the rats (Fig. 6). The V_{max} at 23 mos was 23% lower than that at 6 mos ($p=0.014$, t-test), and the V_{max} at 34 mos was 39% below that at 6 mos ($p=0.012$, t-test), with no significant ($p>0.50$) changes in the K_{act} for Ca^{2+} (Table 3). The reductions in the V_{max} values for activity were considerably greater than the reductions in the levels of the PMCA protein associated with the rafts at the three different ages. These data are quite similar to those we obtained previously with aging SPMs that were not fractionated into rafts and non-rafts (Zaidi et al. 1998).

The PMCA activity shown in figure 6 was determined without the addition of exogenous CaM. As indicated previously, the rafts contain tightly bound CaM; therefore it seemed possible that a partial loss of CaM from the aged rafts could lead to the lower V_{max} of the PMCA activity we observed in those rafts. To address this issue, we used immunoblots and densitometric analyses to determine the relative levels of CaM present in the rafts obtained from rats at the 3 ages. The amount of CaM present in the raft fractions showed no significant age-related decrease. The densitometric units for CaM in rafts isolated from the brains of 6 mos-old rats were 3.4 (± 0.17) $\times 10^7$, that for rafts from 23 mo-old was 3.0 (± 0.05) $\times 10^7$, and those from 34 mo-old 3.1 (± 0.15) $\times 10^7$.

To determine if the addition of exogenous CaM could overcome the age-dependent decrease in PMCA activity in rafts, we measured the PMCA activity of rafts following the addition of exogenous CaM (300 nM) to preparations from brains of rats 6, 23, and 34 mos old. The V_{max} values for the raft PMCA are shown in Table 3. The magnitude of the reductions in the V_{max} values in the aging rafts was not reversed by the CaM addition. Thus the age-dependent decrease in PMCA activity in the rafts did not appear to be due to inadequate levels of CaM, an observation consistent with our results from SPMs (Zaidi et al., 1998). The presence of CaM in the enzyme assays also brought about modest but non-significant ($p=0.10$, t-test) decreases in the K_{act} for Ca^{2+} (Table 3).

Discussion

The hypothesis that Ca^{2+} dysregulation is a fundamental contributor to the progressive decline in cognitive function with age is supported by numerous studies demonstrating changes in several protein systems responsible for neuronal Ca^{2+} signaling as reviewed recently (Kumar et al. 2009). Clearly our observations on the effects of aging on the PMCA system represent only one component of a very complex process, but the marked reduction in the activity of this critical regulator of free intracellular Ca^{2+} concentrations in the synaptic region is likely to be quite significant for overall cognitive performance. The importance of PMCA in regulating Ca^{2+} levels at the synapse is surmised from the demonstration in previous studies of the localization of PMCA isoforms and of specific splice variants of these isoforms in the plasma membrane of dendrites (Marcos et al. 2009; Kenyon et al. 2010) and, importantly, at the subsynaptic web of neuronal synapses (Burette et al. 2010). Furthermore, activation of synaptic Ca^{2+} entry into neurons through glutamate receptors leads to long-term effects on PMCA activity that differ markedly from those induced by general depolarization of neurons (Ferragamo et al. 2009). The studies presented here provide a more detailed picture of the properties of the PMCA in synaptic membranes and support the assertion that the protein does exist in both raft and non-raft domains, that approximately 60% of synaptic membrane PMCA protein is within raft domains, which is

nearly twice the amount of the estimated total synaptic membrane protein distributed in rafts, and, moreover, that the most active pool of PMCA is that present in the rafts. The V_{max} for Ca^{2+}-activated PMCA in rafts was 2.6 and 4.6 times the values in non-raft fractions #5–6 and #7–9 respectively in the young rat brains. The reasons for the high levels of PMCA that is associated with the raft domains in synaptic membranes, and for the even higher activity of the enzyme than could be accounted by the differential distribution of the protein, are not known.

It seems quite likely that the higher specific activity in the rafts is due to the more highly ordered lipid environment in which the protein is embedded. The high cholesterol content and the sphingolipids with saturated acyl chains create a lipid domain that is more ordered than that found in the phospholipid bilayers with unsaturated acyl chains. This higher degree of order has been reported to enhance significantly the PMCA activity of the human ocular lens (Tang et al. 2006) and the red blood cell PMCA reconstituted in lipid vesicles (Zhang et al., 2005). These authors speculate that the enhanced activity is due to the lipid stabilization of the active conformation of the enzyme formed during the catalytic cycle. The sub-plasmalemmal actin filaments that promote lipid-lipid, lipid-protein, and protein-protein interactions within the rafts (Simons and Gerl, 2010) may also contribute to the markedly higher PMCA in these micro-domains.

The present studies, for the first time, have precisely quantified total PMCA as well as the PMCA isoform distribution in raft and non-raft domains of SPMs. Previous studies reported that raft domains in SPMs isolated from pig cerebellum contained only a single isoform of PMCA, the PMCA4 isoform (Sepulveda et al. 2006). This conclusion was based on the relative immunoreactivities of SPM subfractions with PMCA antibodies. The same technique was also used to demonstrate the presence of PMCA4 in raft domains in intestinal smooth muscle (El-Yazbi et al. 2008). However, in MDCK kidney cells, the localization of PMCA2 in apical membranes has been traced to the association of the PMCA2 isoform with lipid raft domains (Xiong et al. 2009). In our studies with rafts isolated from whole rat brains, we unequivocally identified all four isoforms of PMCA in raft domains, as well as in non-raft domains, using both LC-MS/MS as well as immunoblot methodologies. Furthermore, using quantitative MS techniques we were able to estimate the stoichiometric ratios for the four isoforms and to demonstrate that the most abundant forms of PMCA were PMCA4, PMCA2, and PMCA1, with PMCA3 lagging behind the other isoforms in terms of overall levels in rafts and non-raft domains. Therefore, there was no apparent exclusivity for PMCA4 localization in raft domains.

An interesting observation made in the present studies was the tight binding of endogenous CaM to the rafts isolated following treatment of SPMs with the Brij98 detergent and subsequent subfractionation on sucrose density gradients. Whereas treatment of synaptosomes and SPMs with 3 mM EDTA did bring about a decrease in raft-associated CaM and a decrease in PMCA activity, it did not deplete completely the raft-bound CaM. The interaction of raft-bound CaM with the PMCA in these lipid domains was confirmed by the fact that high concentrations of either calmidazolium or trifluoperazine partially inhibited the activity of PMCA and that such inhibition could be completely overcome by the addition of excess exogenous CaM. The residual activity of PMCA in the presence of inhibitors may be the result of remaining high affinity interactions between CaM and PMCA or of the relative abundance of PMCA2 in rafts, an isoform which is minimally affected by the presence of CaM (Brini and Carafoli 2009).

When we assessed the effects of aging on the PMCA activity in the raft fractions, we observed a statistically significant reduction in the V_{max} values of the activity in the rafts at both 23 and 34 months, a reduction in activity that was in excess of the age-associated

decreases in the levels of the PMCA protein in the rafts. The K_{act} for Ca^{2+} did not change with age. Furthermore, the amount of CaM associated with the rafts at the 3 ages showed no significant changes, and the addition of exogenous CaM did not reverse the reduction in activity in the rafts at 34 mos. As lipid raft microdomains are considered to be sites within which receptors and transport carriers are assembled to form important platforms for membrane signaling and molecular trafficking (Lingwood and Simons 2010), the age-associated decreases in SPM raft-associated PMCA levels and activity may strongly influence neuronal handling of Ca^{2+} transients.

In addition to the significant reduction in the V_{max} values of the PMCA activity, we did observe a relatively small but statistically significant increase in the cholesterol to protein ratio in the rafts. This progressive increase from 6 mos to 23 mos, and to 34 mos represents an alteration that would be expected to increase the order within the lipid environment. Cholesterol is present in both leaflets of the membrane bilayer, with 85% distributed into the cytofacial leaflet (Wood et al. 2011). It fills the space under the head groups of sphingolipids or extends the interdigitating fatty acyl chain in the apposing leaflet (Simons and Ikonen 1997). Biochemical and cell-biological experiments have identified cholesterol as an important component of lipid rafts for stability and organization based on the interaction of cholesterol with different membrane lipids (Silvius 2003). If the brain neurons do increase the cholesterol in the aging rafts, it is conceivable that the cells are attempting to make some compensatory response that might increase order and keep the PMCA more active as other age-related processes lead to a significant loss of enzyme activity.

As mentioned in the Introduction, several different mechanisms may contribute to the reduction in PMCA activity without a comparable reduction in levels of the protein. Given our observations that PMCA is uniquely sensitive to inactivation under conditions of oxidative stress (Zaidi and Michaelis 1999), it is quite possible that the protein *per se* could be oxidatively modified and thereby operate much less efficiently. Subtle alterations in the lipid milieu, oxidation of some of the lipids, disruption of interactions between PMCA and some of its numerous protein binding partners (DeMarco and Strehler 2001; Sgambato-Faure et al. 2006), or the state of phosphorylation of specific isoforms such as the tyrosine phosphorylation of PMCA4 (Ghosh et al. 2011) could also influence the enzymatic activity with increasing age. Detailed analyses of possible oxidative modifications of the PMCA and its binding partners in synaptic membranes and of the presence and activity of tyrosine kinases in these membrane fractions are currently underway as we attempt to determine why the contribution of this critical transporter is compromised in the aging brain.

Supplementary Material

Refer to Web version on PubMed Central for supplementary material.

Acknowledgments

This work was supported by NIH grants P01-AG12993 and P30-AG035982.

LJ performed PMCA assays and prepared the first draft of the manuscript. MB prepared SPMs and rafts and carried out lipid measurements and immunoblots. NG and TDW designed and executed all the mass spectrometry studies and analyzed the results of such studies. EKM helped with the experimental design and data analyses, and MLM designed the studies and finalized the manuscript.

Abbreviations used

ACN acetonitrile

AGC	automatic gain control
BSA	bovine serum albumen
CaM	calmodulin
CTXB	cholera toxin subunit B
ESI	electron spray ionization
FLT-1	Flotillin-1
LC-MS	liquid chromatography-mass spectrometry
mos	months
PAGE	Polyacrylamide gel electrophoresis
PVDF	Polyvinylidene fluoride
PMCA	plasma membrane Ca^{2+}-ATPase
SIM	selective ion monitoring
SDS	sodium dodecyl sulfate
SPM	synaptic plasma membranes

References

Berridge MJ. Neuronal calcium signaling. Neuron. 1998; 21:13–26. [PubMed: 9697848]

Blackstone C, Sheng M. Postsynaptic calcium signaling microdomains in neurons. Front Biosci. 2002; 7:d872–885. [PubMed: 11897549]

Brini M, Carafoli E. Calcium pumps in health and disease. Physiol Rev. 2009; 89:1341–1378. [PubMed: 19789383]

Brown DA, London E. Structure of detergent-resistant membrane domains: does phase separation occur in biological membranes? Biochemical and biophysical research communications. 1997; 240:1–7. [PubMed: 9367871]

Burette AC, Strehler EE, Weinberg RJ. A plasma membrane Ca2+ ATPase isoform at the postsynaptic density. Neuroscience. 2010; 169:987–993. [PubMed: 20678993]

Camandola S, Mattson MP. Aberrant subcellular neuronal calcium regulation in aging and Alzheimer's disease. Biochim Biophys Acta. 2011; 1813:965–973. [PubMed: 20950656]

Clapham DE. Calcium signaling. Cell. 2007; 131:1047–1058. [PubMed: 18083096]

DeMarco SJ, Strehler EE. Plasma membrane Ca2+-atpase isoforms 2b and 4b interact promiscuously and selectively with members of the membrane-associated guanylate kinase family of PDZ (PSD95/Dlg/ZO-1) domain-containing proteins. J Biol Chem. 2001; 276:21594–21600. [PubMed: 11274188]

Di Leva F, Domi T, Fedrizzi L, Lim D, Carafoli E. The plasma membrane Ca2+ ATPase of animal cells: structure, function and regulation. Arch Biochem Biophys. 2008; 476:65–74. [PubMed: 18328800]

Duan J, Zhang J, Zhao Y, Yang F, Zhang X. Ganglioside GM2 modulates the erythrocyte Ca2+-ATPase through its binding to the calmodulin-binding domain and its 'receptor'. Arch Biochem Biophys. 2006; 454:155–159. [PubMed: 16962990]

El-Yazbi AF, Cho WJ, Schulz R, Daniel EE. Calcium extrusion by plasma membrane calcium pump is impaired in caveolin-1 knockout mouse small intestine. Eur J Pharmacol. 2008; 591:80–87. [PubMed: 18634779]

Ferragamo MJ, Reinardy JL, Thayer SA. Ca2+-Dependent, Stimulus-Specific Modulation of the Plasma Membrane Ca2+ Pump in Hippocampal Neurons. J Neurophysiol. 2009; 101:2563–2571. [PubMed: 19244356]

Ghosh B, Li Y, Thayer SA. Inhibition of the plasma membrane Ca2+ pump by CD44 receptor activation of tyrosine kinases increases the action potential afterhyperpolarization in sensory neurons. J Neurosci. 2011; 31:2361–2370. [PubMed: 21325503]

Gibson GE, Peterson C. Calcium and the aging nervous system. Neurobiol Aging. 1987; 8:329–343. [PubMed: 3306433]

Gil C, Cubi R, Blasi J, Aguilera J. Synaptic proteins associate with a sub-set of lipid rafts when isolated from nerve endings at physiological temperature. Biochemical and biophysical research communications. 2006; 348:1334–1342. [PubMed: 16920068]

Hering H, Lin CC, Sheng M. Lipid rafts in the maintenance of synapses, dendritic spines, and surface AMPA receptor stability. J Neurosci. 2003; 23:3262–3271. [PubMed: 12716933]

Huidobro A, Blanco P, Villalba M, Gomez-Puertas P, Villa A, Pereira R, Bogonez E, Martinez-Serrano A, Aparicio JJ, Satrustegui J. Age-related changes in calcium homeostatic mechanisms in synaptosomes in relation with working memory deficiency. Neurobiol Aging. 1993; 14:479–486. [PubMed: 8247230]

Jiang L, Fernandes D, Mehta N, Bean JL, Michaelis ML, Zaidi A. Partitioning of the plasma membrane Ca(2+)-ATPase into lipid rafts in primary neurons: effects of cholesterol depletion. J Neurochem. 2007; 102:378–388. [PubMed: 17596212]

Jiang L, Fang J, Moore DS, Gogichaeva NV, Galeva NA, Michaelis ML, Zaidi A. Age-associated changes in synaptic lipid raft proteins revealed by two-dimensional fluorescence difference gel electrophoresis. Neurobiol Aging. 2010; 31:2146–2159. [PubMed: 19118924]

Keller A, Nesvizhskii AI, Kolker E, Aebersold R. Empirical statistical model to estimate the accuracy of peptide identifications made by MS/MS and database search. Analytical chemistry. 2002; 74:5383–5392. [PubMed: 12403597]

Kenyon KA, Bushong EA, Mauer AS, Strehler EE, Weinberg RJ, Burette AC. Cellular and subcellular localization of the neuron-specific plasma membrane calcium ATPase PMCA1a in the rat brain. J Comp Neurol. 2010; 518:3169–3183. [PubMed: 20575074]

Khachaturian ZS. Calcium hypothesis of Alzheimer's disease and brain aging. Ann N Y Acad Sci. 1994; 747:1–11. [PubMed: 7847664]

Kumar A, Bodhinathan K, Foster TC. Susceptibility to Calcium Dysregulation during Brain Aging. Front Aging Neurosci. 2009; 1:2. [PubMed: 20552053]

Landfield PW, Pitler TA. Prolonged Ca2+-dependent afterhyperpolarizations in hippocampal neurons of aged rats. Science. 1984; 226:1089–1092. [PubMed: 6494926]

Lanzetta PA, Alvarez LJ, Reinach PS, Candia OA. An improved assay for nanomole amounts of inorganic phosphate. Anal Biochem. 1979; 100:95–97. [PubMed: 161695]

Lingwood D, Simons K. Lipid rafts as a membrane-organizing principle. Science. 2010; 327:46–50. [PubMed: 20044567]

Lucero HA, Robbins PW. Lipid rafts-protein association and the regulation of protein activity. Arch Biochem Biophys. 2004; 426:208–224. [PubMed: 15158671]

Marcos D, Sepulveda MR, Berrocal M, Mata AM. Ontogeny of ATP hydrolysis and isoform expression of the plasma membrane Ca(2+)-ATPase in mouse brain. BMC Neurosci. 2009; 10:112. [PubMed: 19735545]

Martinez-Serrano A, Blanco P, Satrustegui J. Calcium binding to the cytosol and calcium extrusion mechanisms in intact synaptosomes and their alterations with aging. J Biol Chem. 1992; 267:4672–4679. [PubMed: 1531657]

Martinez A, Vitorica J, Satrustegui J. Cytosolic free calcium levels increase with age in rat brain synaptosomes. Neurosci Lett. 1988; 88:336–342. [PubMed: 3386880]

Mattson MP. Calcium and neurodegeneration. Aging Cell. 2007; 6:337–350. [PubMed: 17328689]

Michaelis EK, Michaelis ML, Chang HH, Kitos TE. High affinity Ca2+-stimulated Mg2+-dependent ATPase in rat brain synaptosomes, synaptic membranes, and microsomes. J Biol Chem. 1983; 258:6101–6108. [PubMed: 6133858]

Michaelis ML. Ca2+ handling systems and neuronal aging. Ann N Y Acad Sci. 1989; 568:89–94. [PubMed: 2629587]

Michaelis ML, Johe K, Kitos TE. Age-dependent alterations in synaptic membrane systems for Ca2+ regulation. Mech Ageing Dev. 1984; 25:215–225. [PubMed: 6144821]

Michaelis ML, Foster CT, Jayawickreme C. Regulation of calcium levels in brain tissue from adult and aged rats. Mech Ageing Dev. 1992; 62:291–306. [PubMed: 1583914]

Olsen JV, Mann M. Improved peptide identification in proteomics by two consecutive stages of mass spectrometric fragmentation. Proc Natl Acad Sci U S A. 2004; 101:13417–13422. [PubMed: 15347803]

Sepulveda MR, Berrocal-Carrillo M, Gasset M, Mata AM. The plasma membrane Ca2+-ATPase isoform 4 is localized in lipid rafts of cerebellum synaptic plasma membranes. J Biol Chem. 2006; 281:447–453. [PubMed: 16249176]

Sgambato-Faure V, Xiong Y, Berke JD, Hyman SE, Strehler EE. The Homer-1 protein Ania-3 interacts with the plasma membrane calcium pump. Biochemical and biophysical research communications. 2006; 343:630–637. [PubMed: 16554037]

Silvius JR. Role of cholesterol in lipid raft formation: lessons from lipid model systems. Biochim Biophys Acta. 2003; 1610:174–183. [PubMed: 12648772]

Simons K, Ikonen E. Functional rafts in cell membranes. Nature. 1997; 387:569–572. [PubMed: 9177342]

Simons K, Toomre D. Lipid rafts and signal transduction. Nat Rev Mol Cell Biol. 2000; 1:31–39. [PubMed: 11413487]

Strehler EE, Zacharias DA. Role of alternative splicing in generating isoform diversity among plasma membrane calcium pumps. Physiol Rev. 2001; 81:21–50. [PubMed: 11152753]

Tang D, Dean WL, Borchman D, Paterson CA. The influence of membrane lipid structure on plasma membrane Ca2+-ATPase activity. Cell Calcium. 2006; 39:209–216. [PubMed: 16412504]

Wood WG, Igbavboa U, Muller WE, Eckert GP. Cholesterol asymmetry in synaptic plasma membranes. J Neurochem. 2011; 116:684–689. [PubMed: 21214553]

Xiong Y, Antalffy G, Enyedi A, Strehler EE. Apical localization of PMCA2w/b is lipid raft-dependent. Biochemical and biophysical research communications. 2009; 384:32–36. [PubMed: 19379709]

Zaidi A, Michaelis ML. Effects of reactive oxygen species on brain synaptic plasma membrane Ca(2+)-ATPase. Free Radic Biol Med. 1999; 27:810–821. [PubMed: 10515585]

Zaidi A, Gao J, Squier TC, Michaelis ML. Age-related decrease in brain synaptic membrane Ca2+-ATPase in F344/BNF1 rats. Neurobiol Aging. 1998; 19:487–495. [PubMed: 9880051]

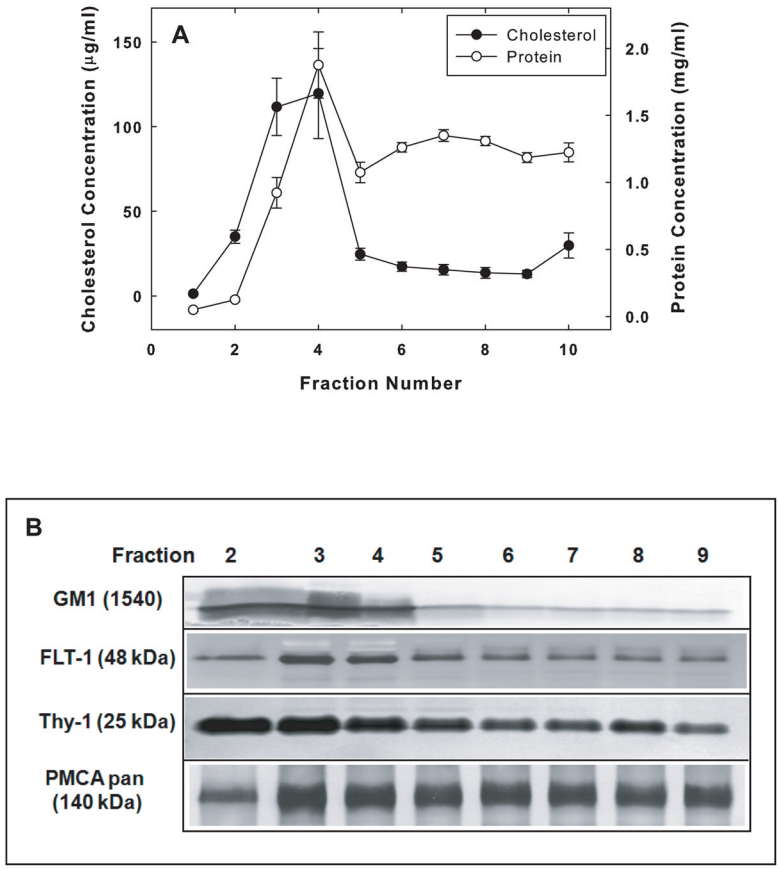

Fig. 1.

Characterization of raft and non-raft domains isolated from SPMs of 6-mos F344/BNF1 rat brains. **(A)** Analysis of cholesterol and protein content of the 10 fractions collected from the sucrose density gradient as described under Methods. Data are means ± SEM obtained from 6 animals. **(B)** Cholera toxin and immunoblot detection of raft markers and PMCA. Eight μg of protein from fractions 2–9 were loaded on the gel for GM1, FLT-1, and pan PMCA detection, and 15 μg of protein for Thy-1 detection. The GM1 was detected with cholera toxin as described in the Methods. The dilutions for the various antibodies were: FLT-1 (1:250), Thy-1 (1:250), and pan PMCA (1:1000). Representative blots from 3 independent experiments with similar results are shown.

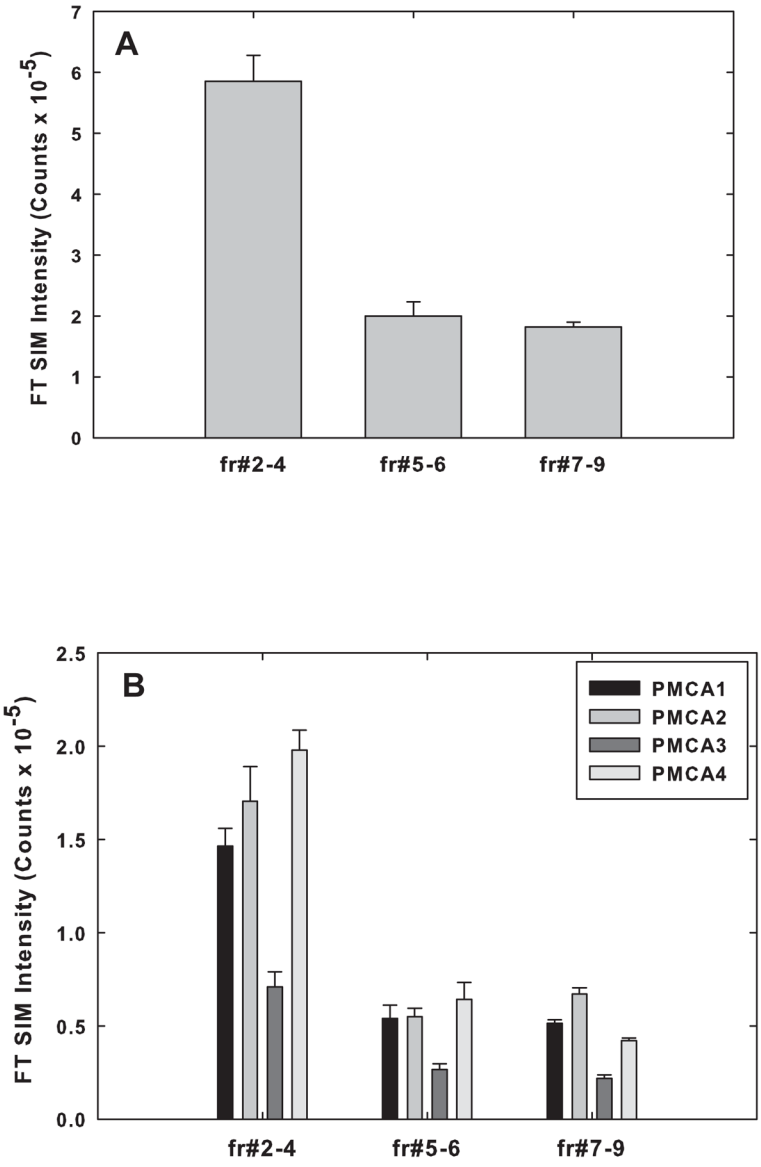

Fig. 2.

Distribution of the total PMCA protein and the PMCA isoforms in the raft and non-raft fractions from rats at 6 mos as determined by quantitative mass spectrometry described under Methods. **(A)** The total FT SIM intensity counts based on LC-MS/MS analysis of the 4 isoforms in each of the pooled fractions (#2–4, #5–6, #7–9), were added and the percentage of the total membrane PMCA present in each of the fractions calculated. **(B)** Quantitative FT SIM mass spectrometric measurements of PMCA isoform-specific peptides present in each of the 3 fractions are shown. Data are presented as the means ± SEM of triplicate determinations from 2 preparations.

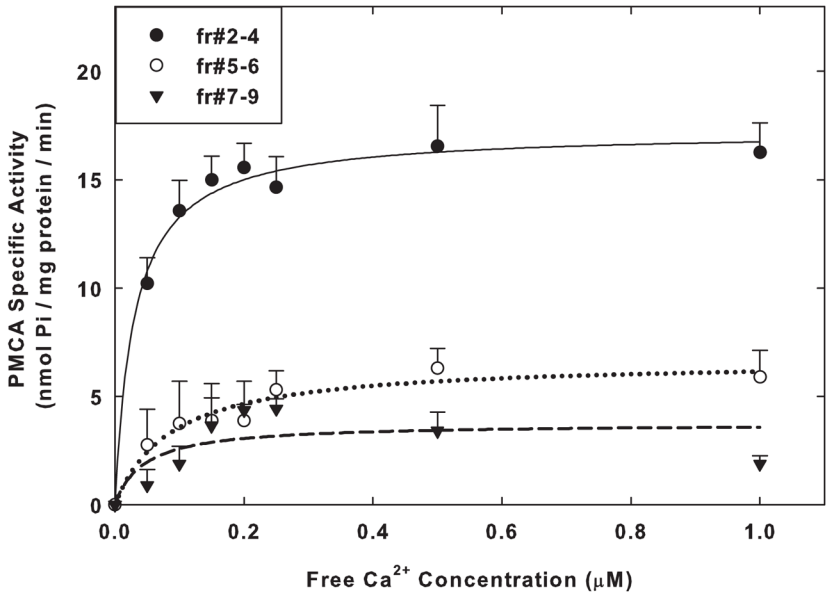

Fig. 3.

Measurement of the specific activity of PMCA in the raft and non- raft fractions. Fractions #2–4, #5–6, and #7–9 were pooled, and 3 μg of protein from each was assayed for PMCA activity across Ca^{2+} concentrations as described under Methods. The activities were determined in the absence of exogenous CaM. Each point is the mean ± SEM of triplicate determinations of the specific activity in nmol P_i/mg protein/min for the raft and non-raft fractions obtained from the SPMs isolated from 5 animals at 6 mos of age. Curves were plotted with least squares fitting of the data to the Michaelis-Menten equation using Sigma Plot 11. The V_{max} and K_{act} values determined in the presence and absence of saturating levels of exogenous CaM are listed in Table 2.

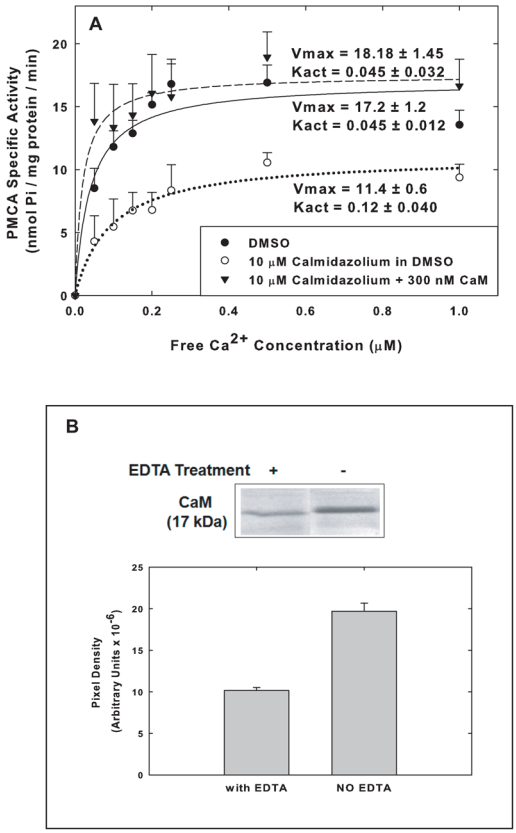

Fig. 4.

Effects of the CaM inhibitor Calmidazolium and EDTA extraction of CaM on the specific activity of PMCA in raft and non-raft fractions. **(A)** Raft and non-raft fractions were pre-incubated and assayed with 1% DMSO only (final concentration), 10 μmM Calmidazolium in DMSO, or 10μM Calmidazolium in DMSO + 300 nM CaM, and the specific activity was measured across Ca^{2+} concentrations. The V_{max} and K_{act} values calculated from 4 membrane preparations are shown in the figure. Statistical analysis of V_{max} and K_{act} values for the Calmidazolium *vs* Calmidazolium + CaM yielded $p < 0.005$ and $p < 0.12$ respectively. **(B)** CaM remaining in rafts after extraction with 3 mM EDTA. Synaptosomes were exposed to 3 mM EDTA during lysis as described in the Methods and 15 μg of protein from Fr #2–4 were run on SDS-PAGE, transferred, and probed with antibodies to CaM. The immunoblot shown is representative of 6 similar blots.

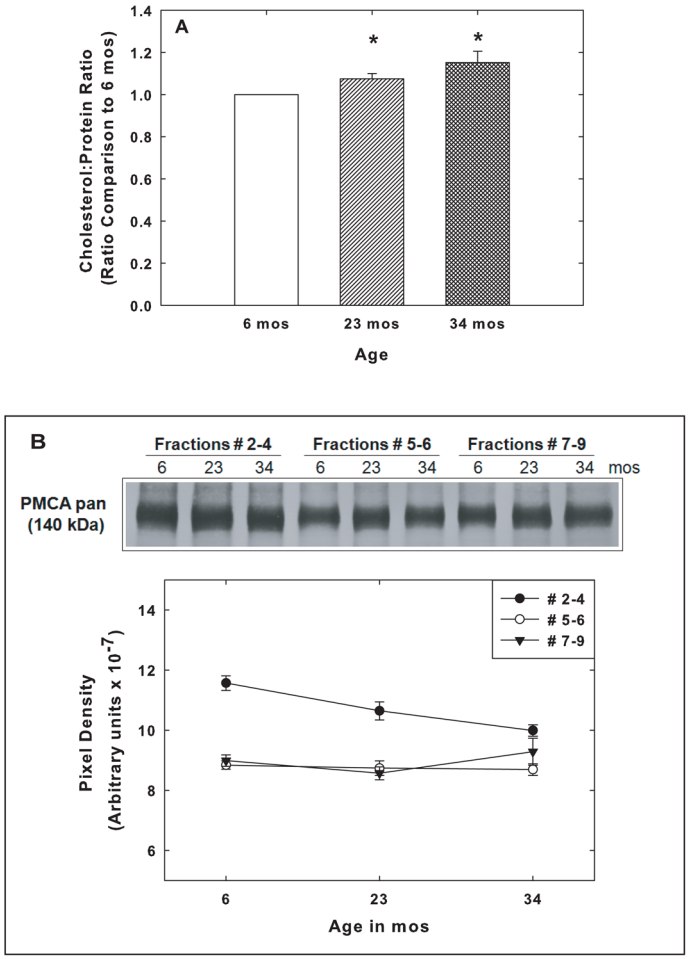

Fig. 5.

Effects of aging on cholesterol to protein ratios and on PMCA levels in rafts and non-raft fractions. **(A)** Rafts (fractions #2–4) were collected from animals at 6, 23, and 34 mos. The total cholesterol was determined with Amplex Red and the bicinchoninic assay was used to determine the total protein in each sample. The cholesterol to protein ratio for the rafts at 6 mos was set to 1.0, and the ratios for the 23 and 34 mos samples calculated relative to the 6 mos value. Data represent the means ± SEM of the ratios from 5 sets of animals, and the significance of differences between samples were assessed by Student's *t* test. ***** = $p < 0.02$. **(B)** Immunoblot analysis of PMCA levels was carried out with the pan PMCA antibody on pooled fractions #2–4, #5–6, and #7–9, prepared from the SPMs of 6, 23, and 34 mos F344BNF1 rat brains. **(C)** Relative immunoreactivities with the pan PMCA antibody were quantified in the fractions from 5 sets of animals, and the means ± SEM are shown. One-way Anova analysis revealed a statistically significant age effect ($p<0.03$) on PMCA levels in the raft fraction (#2–4) though the levels of the protein are higher than in the non – raft fractions. PMCA levels in the 2 non-raft fractions showed no significant change with age.

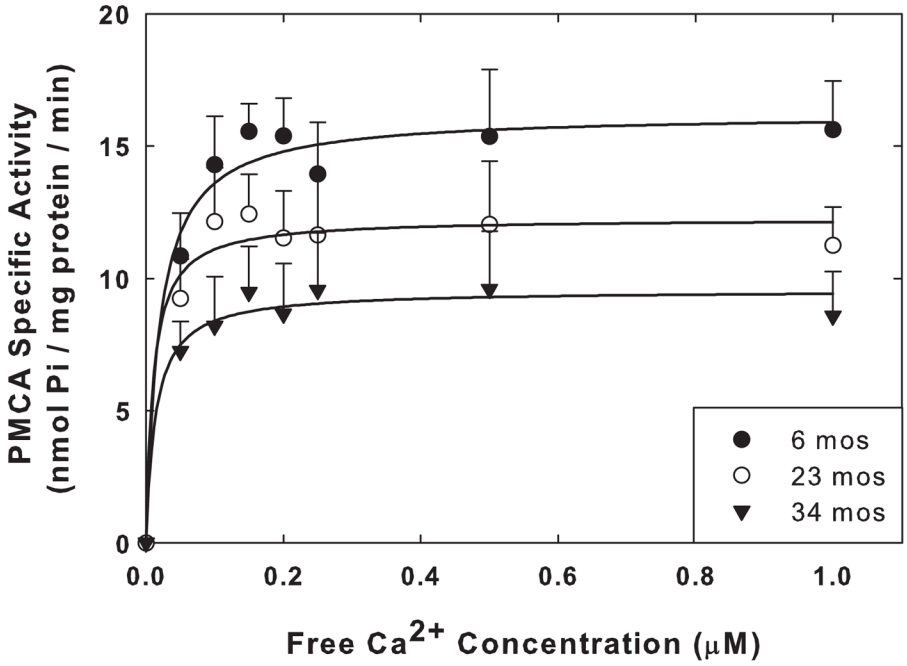

Fig. 6.

Effects of aging on the specific activity of PMCA in the raft fractions (#2–4) assayed without the addition of exogenous CaM. Each point is the mean ± SEM of triplicate determinations of the specific activity in nmol P_i/mg protein/min for the raft fractions obtained from the SPMs isolated from 4 sets of animals at 6, 23, and 34 mos of age. Curves were plotted with least squares fitting of the data to the Michaelis-Menten equation using Sigma Plot 11. The V_{max} and K_{act} values determined in the presence and absence of saturating levels of exogenous CaM are listed in Table 3.

Table 1

Stoichiometric ratios of PMCA isoforms in pooled fractions #2–4, 5–6, and 7–9[a].

Pooled Fractions[b]	PMCA1[c]	PMCA2[c]	PMCA3[c]	PMCA4[c]
2 – 4	0.251±0.013	0.289±0.038	0.119±0.015	0.341±0.031
5 – 6	0.269±0.021	0.278±0.020	0.134±0.014	0.319±0.016
7 – 9	0.282±0.012	0.368±0.019	0.119±0.012	0.231±0.015

[a]Stoichiometric ratios of PMCA isoforms were calculated by normalizing the chromatographic areas measured by FT SIM MS to the sum of the areas for the four isoform-specific peptides.

[b]Pooled fractions were isolated by Brij98 treatment of SPMS followed by sucrose density centrifugation. Peptides from these fractions were obtained following protein digestion of proteins separated by SDS gel electrophoresis as described under Methods.

[c]Values represent the mean ± SD of 6 sample determinations.

Table 2

Summary of constants V_{max} and K_{act} of PMCA activity in raft and non-raft fractions of SPMs isolated from 6 mos old rat brain and measured in the presence or absence of exogenous CaM.

Pooled Fractions[a]	V_{max} (nmol Pi mg^{-1} protein min^{-1})[b]		K_{act} (μM)	
	No CaM	Plus CaM[c]	No CaM	Plus CaM[c]
2 – 4	16.7 ± 0.8	16.8 ± 0.7	0.023 ± 0.004	0.011 ± 0.006
5 – 6	7.4 ± 1.2	7.7 ± 1.4	0.088 ± 0.059	0.065 ± 0.037
7 – 9	4.1 ± 0.5	3.9 ± 0.1	0.049 ± 0.042	0.046 ± 0.040

[a] PMCA activity was measured in pooled fractions isolated by Brij98 treatment of SPMS followed by sucrose density centrifugation.

[b] Values represent the mean ± SEM of constants obtained from the analyses of Michaelis-Menten fitting of the data from 5 rats per group (all measurements performed in triplicate).

[c] The concentration of CaM added was 300 nM.

Table 3

Summary of constants V_{max} and K_{act} of PMCA activity in raft domains isolated from SPMs from 6, 23, and 34 mos old rats and measured in the presence or absence of exogenous CaM.

Age (Months)	V_{max}[a] (nmol Pi mg^{-1} protein min^{-1})[b]		K_{act}[a] (μM)	
	No CaM	Plus CaM[c]	No CaM	Plus CaM[c]
6	17.5 ± 0.6	16.5 ± 0.8	0.033 ± 0.005	0.015 ± 0.007
23	13.4 ± 1.1	13.5 ± 0.5	0.026 ± 0.008	0.0078 ± 0.01
34	10.7 ± 1.8	10.8 ± 1.1	0.037 ± 0.01	0.011 ± 0.004

[a] PMCA activity measured as described in Table 2.

[b] Values represent the mean ± SEM of constants obtained from the analyses of Michaelis-Menten fitting of the data from 4 rats per group (all measurements performed in triplicate).

[c] The concentration of CaM added was 300 nM.